



Deposited via The University of Sheffield.

White Rose Research Online URL for this paper:

<https://eprints.whiterose.ac.uk/id/eprint/105387/>

Version: Accepted Version

Article:

Ely, J., Gribble, E. and Clark, C.D. (2016) The glacial geomorphology of the western cordilleran ice sheet and Ahklun ice cap, Southern Alaska. *Journal of Maps*, 12 (Supp 1). pp. 415-424. ISSN: 1744-5647

<https://doi.org/10.1080/17445647.2016.1234981>

Reuse

Items deposited in White Rose Research Online are protected by copyright, with all rights reserved unless indicated otherwise. They may be downloaded and/or printed for private study, or other acts as permitted by national copyright laws. The publisher or other rights holders may allow further reproduction and re-use of the full text version. This is indicated by the licence information on the White Rose Research Online record for the item.

Takedown

If you consider content in White Rose Research Online to be in breach of UK law, please notify us by emailing eprints@whiterose.ac.uk including the URL of the record and the reason for the withdrawal request.

1 **The Glacial Geomorphology of the Western Cordilleran Ice Sheet and Ahklun Ice**

2 **Cap, Southern Alaska**

3 Jeremy C. Ely *, Emily, A. Gribble and Chris D. Clark

4 *Department of Geography, The University of Sheffield, Winter Street, Sheffield, S10 2TN, UK*

5 *corresponding author: j.ely@sheffield.ac.uk

6 **Abstract**

7 During the late Wisconsinan, Southern Alaska was covered by two large ice masses; the
8 western arm of the Cordilleran Ice Sheet and the Ahklun Mountains Ice Cap. Compared to the
9 other ice sheets that existed during this period (e.g., the British-Irish, Laurentide and
10 Fennoscandian ice sheets), little is known about the geomorphology they left behind. This limits
11 our understanding of their flow pattern and retreat. Here we present systematic mapping of the
12 glacial geomorphology of the two ice masses which existed in Southern Alaska. Due to spatially
13 variable data availability, mapping was conducted upon digital elevation models and satellite
14 images of varying resolutions. Offshore, we map the glacial geomorphology using available
15 bathymetric data. For the first time, we document > 5000 subglacial lineations, recording ice
16 flow direction. The distribution of moraines is presented, as well as features related to glacial
17 meltwater drainage patterns (eskers and meltwater channels). Prominent troughs were also
18 mapped on Alaska's continental shelf. This map provides the data required for a glacial inversion
19 of these palaeo-ice masses.

20 **1. Introduction**

21 Approximately 70,000 km² (5%) of Alaska is currently glaciated (Molnia, 2008). During
22 the late Wisconsinan (~30 to 10 kya) ice extent was approximately 10 times greater than this,
23 with previous glaciations greater still in extent (Kaufman and Manley, 2004; Kaufman et al.,
24 2011). The majority of this ice was contained within three ice masses; an ice cap over the Brooks
25 range to the north of Alaska (Hamilton and Porter, 1975), a second ice cap over the Ahklun
26 Mountains (Briner and Kaufman, 2000) and a much larger ice sheet in the south. The latter
27 formed the Western edge of the Cordilleran ice sheet at its maximum (Booth et al., 2004) and

28 covered the Aleutian Islands in the West, the Alaskan Peninsula and the Wrangell Mountains in
29 the East (Mann and Peteet, 1994; Kaufman et al., 2011). As well as containing a large volume of
30 fresh water, these Alaskan ice masses may have formed a barrier to human migration across the
31 land bridge, known as Beringia, which existed between Alaska and Russia during the last glacial
32 period (Mandryk et al., 2001; Misarti et al., 2012). Figure 1 shows the proposed extent of ice at
33 different times across southern Alaska. This paper focuses upon the geomorphology left behind
34 by the two principle ice masses in this area; the Ahklun Mountains Ice Cap and the Western
35 Cordilleran Ice Sheet (Figure 1).

36 The maximum extent of the Alaskan ice masses has been proposed and mapped (e.g.,
37 Figure 1, Kaufman and Manley, 2004; Kaufman et al., 2011), but less is known about the pattern
38 of the retreat of these ice masses. This is partially due to a lack of a map of the glacial landforms
39 which this ice sheet left behind. The distribution of moraines, meltwater channels, glacial
40 troughs, eskers and subglacial bedforms can be used to reconstruct ice sheets via a glacial
41 inversion method (e.g., Kleman and Borgström, 1996, Clark, 1999; Stokes et al., 2015). This
42 technique has proven informative for the British-Irish (e.g., Greenwood and Clark, 2008; Hughes
43 et al., 2010; Clark et al., 2012), Fennoscandian (e.g., Kleman et al., 1997; Stroeven et al., 2015),
44 Cordilleran (e.g., Margold et al., 2013) and Laurentide ice sheets (e.g., Boulton and Clark,
45 1990b; Trommelen et al., 2014). Here we present mapping of the glacial geomorphology for the
46 Ahklun Mountains Ice Cap and the Western Cordilleran Ice Sheet across the area they each
47 encompassed during the late Wisconsinan. This map will form the basis of an empirical
48 reconstruction of these ice masses.

49 **2. Methods**

50 Onshore, glacial landforms were identified and mapped using three sources of data. All
51 onshore sources were obtained from the USGS website (www.earthexplorer.usgs.gov). The
52 datasets used and their resolution are listed in Table 1. A digital elevation model (DEM) derived
53 from interferometric synthetic aperture radar (IfSAR) provided the highest resolution data (5 m),
54 but is not available across the whole of Alaska (Figure 2). Below 60°N the shuttle radar
55 topography mission DEM (SRTM; 30 m resolution) was used (Figure 2). To fill the space where
56 neither of these two datasets were available, glacial landforms were identified on Landsat ETM+
57 imagery (15 m pan-chromatic resolution), which is available globally. Offshore, elevation
58 models are available from NOAA (<https://maps.ngdc.noaa.gov/viewers/bathymetry/>). DEMs of
59 various resolutions were available (Table 1). Where high resolution bathymetric data was not
60 available, a coarser resolution (500 m) elevation model was used. Only the largest glacial
61 features such as glacial troughs or large moraines (several km's in length and 10's of m in
62 amplitude) were visible on this DEM.

63 To maximise landform identification, we adopted a repeat pass approach to mapping,
64 checking each area multiple times. However, our mapping is necessarily limited where high
65 resolution offshore elevation models are unavailable. Where high resolution data was available,
66 for example the IfSAR DEM (Table 1 and Figure 2), this enabled a high level of identification
67 and subsequent mapping of landforms. As a consequence, these areas are mapped in more detail
68 than others. Therefore, we anticipate more detailed geomorphology may be revealed as higher
69 resolution datasets become available, prompting future work. Landform preservation, burial and
70 submergence also limit landform identification.

71 Glacial landforms were identified on hill-shaded relief models created from the available
72 DEMs. Two hill-shades were created from each DEM, illuminating from 45° and 315° to avoid

73 azimuth biasing (Smith and Clark, 2005; Figure 3A and B). Hill-shades were made semi-
74 transparent and overlaid on a DEM in order to avoid mapping hollows. False colour composite
75 (bands 4, 3 and 2) Landsat images were enhanced using local image statistics in order to
76 highlight subtle topography (e.g. Ely and Clark, 2016). The pan-chromatic band was used to
77 further refine the imagery, to give a horizontal resolution of 15 m (Figure 3C). Features were
78 mapped using a combination of hill-shade illumination angles and satellite data (Figure 3D).

79 The following features were identified and mapped: subglacial lineations, streamlined
80 bedrock, moraines, eskers, meltwater channels and glacial troughs. Subglacial lineations were
81 mapped as polygons around their break of slope. Break of slope was identifiable on hill-shaded
82 DEMs (Hughes et al., 2010; Hiller et al., 2015; Figure 3 A and B). On satellite imagery these
83 breaks of slope were visible as changes in reflection or vegetation (Spagnolo et al., 2014). On the
84 higher resolution IfSAR DEM (Table 1), many streamlined features were qualitatively different
85 in appearance, giving the impression that they were predominately composed of bedrock (e.g.,
86 Bradwell, 2005; Lane et al., 2015; Figure 4). Differentiation of these features was aided by a
87 surface geology map. Where possible, moraines were also mapped as polygons. Often, moraines
88 were composed of several ridges comprising a moraine complex. Where this was the case, the
89 smaller ridges were mapped as polylines and the moraine complex as a polygon (Figure 5).
90 Furthermore, some smaller moraines were mapped solely as polylines along their crest. Eskers
91 were also mapped as polylines along their crestline. Glacial meltwater channels were mapped as
92 polygons along their thalweg. These were identified as glacial in origin due to their discordance
93 with modern day fluvial drainage patterns (c.f. Greenwood et al., 2007). However, it is
94 reasonable to expect that a channel may have been occupied by both a glacially dominated
95 source of water and by a fluvial or glaciofluvial water source at a later stage. Finally, glacial

96 troughs were mapped as polylines along their banks, using 3D profiles and hill-shading to define
97 their edges (Spagnolo and Clark, 2009). Unlike other ice sheets (e.g., Hättestrand and Kleman,
98 1999; Trommelen and Ross, 2010; McHenry and Dunlop, 2015), no examples of subglacial ribs,
99 which form transverse to flow direction, were noted.

100 **3. Map description**

101 The Main Map was produced in ArcGIS 10.1. It is comprised of 12,846 digitised polylines
102 and polygons. The background for the map is a merged bathymetric and terrestrial elevation
103 model downloaded from the National Oceanic and Atmospheric Administration (NOAA,
104 www.ngdc.noaa.gov). The extent of modern day glaciers, available from the Randolph Glacier
105 Inventory (version 5, www.glims.org/RGI/), is also included on the map in order to contrast with
106 landforms created by more extensive glaciers. The map is projected in NAD 1983 CORS96
107 Alaska Albers and is designed to be printed on 2A0 paper, at a scale of 1:1,000,000. The
108 distribution, frequency and characteristics of the mapped glacial landforms are discussed below.

109 *3.1. Subglacial lineations and streamlined bedrock*

110 Despite their frequency both in the literature and upon previously glaciated landscapes, the
111 subglacial bedforms of Alaska have hitherto received little to no mention within the literature.
112 Here, 5878 subglacial lineations, which are formed aligned with flow direction, were mapped
113 from the 4 main sources of data (Table 2). Exemplars were found near Becharof Lake (Figure 3),
114 within McCarthy Borough, Valdez-Cordova (Figure 6A) and at the confluence between the West
115 and East Forks of the Yetna River (Figure 6B). Lineations were also observed in the Akhlun ice
116 cap area (Main Map; Figure 6C), where they record a radial flow pattern outward from the centre

117 of the mountain range and along valley floors. Furthermore, subglacial lineations were also
118 observed on offshore bathymetry (Figure 6D).

119 Subglacial lineations form a morphological continuum of landforms spanning those
120 typically referred to as drumlins, to mega-scale glacial lineations (Ely et al., 2016). The majority
121 of Alaskan subglacial lineations would fall into the shorter end of this continuum, having low
122 length-width ratios and thus conforming to the part of this continuum which is typically referred
123 to as drumlins (Clark et al., 2009). However, a few drumlins are remarkably long, elongate and
124 parallel, reaching lengths above 6 km, exceeding the size of bedforms typically found on ice
125 stream beds (e.g., Figure 6B; Spagnolo et al., 2014). Future work is required to establish the
126 potential role of palaeo-ice streaming across Alaska.

127 Additionally, 1239 examples of subglacially streamlined bedrock landforms were mapped
128 (Table 1). These are typically 500 m long and a few metres high: exemplars are shown on Figure
129 4. These landforms can also be used to infer past flow direction and possible ice streaming (e.g.,
130 Bradwell et al., 2008; Lane et al., 2015), but likely form by a separate set of processes to other
131 subglacial bedforms (Dionne, 1987), hence their separation on our map. Streamlined bedrock is
132 especially prominent on the mountains to the west of the Copper Basin (Figure 4). This suggests
133 that at some point the Cordilleran Ice Sheet covered these mountains.

134 *3.2. Moraines*

135 Moraines were mapped as polylines and polygons (n = 4101) from the different data
136 sources (Table 3). A large range of moraine sizes were observed, the smallest being less than a
137 metre high and a few metres wide, with the larger moraine complexes several tens of metres in
138 height and kilometres wide. Some of the most impressive morainic patterns were found on the

139 northern sides of the Alaskan Peninsula (Figure 7A), the Aleutian Range (Figure 7B) and the
140 Alaska Range (Figure 7C). Impressive moraines were also noted to emanate from the Akhlun
141 mountains (Figures 5 and 7D). Comparatively few moraines were noted offshore, at least
142 partially due to sparse data coverage or burial by post-glacial sediment. Many of the moraines
143 form concentric, looped patterns (Figures 5 and 7) suggesting along valley margin standstills as
144 the ice retreated.

145 *3.3. Eskers and meltwater channels*

146 Eskers were only observed on the IfSAR DEM, either due to the higher resolution of this
147 data, or perhaps eskers were only formed in the region that this DEM covers (Figure 2).
148 Polylines (n = 592) included on the Main Map represent individual esker segments (e.g., Storrar
149 et al., 2014), the shortest of which were a few tens of metres in length, but in places were traced
150 for over 4 km. Compared to the Laurentide (Storrar et al., 2014) and Fennoscandian ice sheets
151 (Stroven et al., 2015) eskers are rare. This perhaps highlights differences in the drainage of these
152 ice sheets, or points toward a poor preservation of eskers in Alaska. An example esker is shown
153 in Figure 8A. As has been reported for other palaeo-ice sheets (Greenwood et al., 2016), eskers
154 were observed to switch into meltwater channels (e.g., Figure 8B), but meltwater channels were
155 also observed in isolation from eskers (e.g., Figure 8C). In total, 1979 meltwater channels were
156 mapped, again ranging from a few tens of metres to several kilometres in length. Future work is
157 required to classify these meltwater channels before they can be used for glacial inversion (e.g.,
158 Greenwood et al., 2007).

159 *3.4. Troughs*

160 Polylines (n= 135) marking the edge of troughs are included on the Main Map. The troughs
161 are typically 50 to 300 m deep, and several hundreds of metres wide. The largest trough forms
162 the Shelikof Strait, between the Aleutian Mountains and Kodiak Island, through which ice has
163 been hypothesised to flow (Mann and Peteet, 1994). Further troughs are evident across the
164 southern Alaskan continental shelf (Figure 9C and D; Schwartz et al., 2015). Elsewhere, ice
165 streams form along such troughs (e.g., the Norwegian channel ice stream (Sejrup et al., 2003)
166 and the Lambert Glacier-Amery ice shelf system (Hambrey and Dowdeswell, 1994)). However,
167 a lack of high resolution bathymetry within the Shelikof Strait, and other troughs, prohibits any
168 recognition of a possible palaeo-ice stream imprint (Stokes and Clark, 1999).

169 **4. Summary and Conclusions**

170 The Cordilleran Ice Sheet and Ahklun Mountains Ice Cap left behind a wealth of
171 geomorphological evidence during the late Wisconsinan in southern Alaska. Here we present the
172 first systematic map of the glacial geomorphology across the areas formally occupied by these
173 ice masses. Our mapping covers the terrestrial portion of these ice sheets, and, where
174 bathymetric data exists, the submerged geomorphology. The map documents numerous
175 subglacial lineations, which may represent the tracks of palaeo-ice streams. Large, looping
176 moraine sequences record the recession of the ice masses. We also note features related to glacial
177 meltwater, channels and eskers, as well as systems of glacial troughs offshore. This map
178 provides the basis for a future empirical reconstruction of the ice masses in this area.

179 **5. Software**

180 Mapping and data manipulation were conducted in ESRI ArcGIS 10.1.

181 **6. Acknowledgements**

182 This work was funded by a Sheffield University Research Experience (S.U.R.E) grant. We
183 would like to thank Danni Pearce, Martin von Wyss, Jakob Heyman, Giedrė Beconytė, Martin
184 Margold and the editors for their useful comments.

185 **Map Design**

186 The Main Map was produced using ArcMap v 10.1. The names of significant mountain ranges,
187 river basins and oceans are included in order to orientate the map user. The background to the
188 map is a semi-transparent DEM, classified to highlight the break of the continental shelf and to
189 show upland regions. Modern day glacier distribution is shown to explain “blank” areas on the
190 map where landforms are masked by ice, and to provide a contrast with the more extensive
191 geomorphology left behind by the last ice sheets in Alaska.

192 **7. References**

193 Booth, D.B., Troost, K.G., Clague, J.J. and Waitt, R.B., 2004. The Cordilleran ice sheet. *The*
194 *Quaternary Period in the United States, 1*, pp.17-43.

195 Boulton, G.S. and Clark, C.D., 1990. The Laurentide ice sheet through the last glacial cycle: the
196 topology of drift lineations as a key to the dynamic behaviour of former ice
197 sheets. *Transactions of the Royal Society of Edinburgh: Earth Sciences*, 81(04), pp.327-
198 347.

199 Bradwell, T., 2005. Bedrock megagrooves in Assynt, NW Scotland. *Geomorphology*, 65(3),
200 pp.195-204.

201 Bradwell, T., Stoker, M. and Krabbendam, M., 2008. Megagrooves and streamlined bedrock in
202 NW Scotland: the role of ice streams in landscape evolution. *Geomorphology*, 97(1),
203 pp.135-156.

204 Briner, J.P. and Kaufman, D.S., 2000. Late Pleistocene glaciation of the southwestern Ahklun
205 mountains, Alaska. *Quaternary Research*, 53(1), pp.13-22.

206 Clark, C.D., 1999. Glaciodynamic context of subglacial bedform generation and
207 preservation. *Annals of Glaciology*, 28(1), pp.23-32.

208 Clark, C.D., Hughes, A.L., Greenwood, S.L., Spagnolo, M. and Ng, F.S., 2009. Size and shape
209 characteristics of drumlins, derived from a large sample, and associated scaling
210 laws. *Quaternary Science Reviews*, 28(7), pp.677-692.

211 Clark, C.D., Hughes, A.L., Greenwood, S.L., Jordan, C. and Sejrup, H.P., 2012. Pattern and
212 timing of retreat of the last British-Irish Ice Sheet. *Quaternary Science Reviews*, 44, pp.112-
213 146.

214 Dionne, J.C., 1987. Tadpole rock (rocdrumlin): a glacial streamline moulded form. In *Drumlin*
215 *Symposium. Rotterdam: Balkema* (Vol. 149, p. 159).

216 Ely, J.C. and Clark, C.D., 2016. Flow-stripes and foliations of the Antarctic ice sheet. *Journal of*
217 *Maps*, 12(2), pp.249-259.

218 Ely, J.C., Clark, C.D., Spagnolo, M., Stokes, C.R., Greenwood, S.L., Hughes, A.L., Dunlop, P.
219 and Hess, D., 2016. Do subglacial bedforms comprise a size and shape
220 continuum?. *Geomorphology*, 257, pp.108-119.

221 Greenwood, S.L., Clark, C.D. and Hughes, A.L., 2007. Formalising an inversion methodology
222 for reconstructing ice-sheet retreat patterns from meltwater channels: application to the
223 British Ice Sheet. *Journal of Quaternary Science*, 22(6), pp.637-645.

224 Greenwood, S.L. and Clark, C.D., 2008. Subglacial bedforms of the Irish ice sheet. *Journal of*
225 *Maps*, 4(1), pp.332-357.

226 Greenwood, S.L., Clason, C.C., Helanow, C. and Margold, M., 2016. Theoretical, contemporary
227 observational and palaeo-perspectives on ice sheet hydrology: Processes and
228 products. *Earth-Science Reviews*, 155, pp.1-27.

229 Hambrey, M.J. and Dowdeswell, J.A., 1994. Flow regime of the Lambert Glacier-Amery Ice
230 Shelf system, Antarctica: structural evidence from Landsat imagery. *Annals of*
231 *Glaciology*, 20(1), pp.401-406.

232 Hamilton, T.D. and Porter, S.C., 1975. Itkillik glaciation in the Brooks Range, northern
233 Alaska. *Quaternary Research*, 5(4), pp.471-497.

234 Hättestrand, C. and Kleman, J., 1999. Ribbed moraine formation. *Quaternary Science*
235 *Reviews*, 18(1), pp.43-61.

236 Hillier, J.K., Smith, M.J., Armugam, R., Barr, I., Boston, C.M., Clark, C.D., Ely, J., Frankl, A.,
237 Greenwood, S.L., Gosselin, L. and Hättestrand, C., 2015. Manual mapping of drumlins in
238 synthetic landscapes to assess operator effectiveness. *Journal of Maps*, 11(5), pp.719-729.

239 Hughes, A.L., Clark, C.D. and Jordan, C.J., 2010. Subglacial bedforms of the last British Ice
240 Sheet. *Journal of Maps*, 6(1), pp.543-563.

241 Kaufman, D.S., Manley, W.F., 2004. Pleistocene maximum and Late Wisconsin glacier extents
242 across Alaska, USA. In: Ehlers, J., Gibbard, P.L. (Eds.), Quaternary Glaciations—Extent
243 and Chronology, Part II: North America. Developments in Quaternary Science, vol. 2
244 Elsevier, Amsterdam, pp. 9–27.

245 Kaufman, D.S., Young, N.E., Briner, J.P. and Manley, W.F., Alaska Palaeo-Glacier Atlas
246 (Version 2). In: Ehlers, J., Gibbard, P.L. and Hughes, P.D. Quaternary Glaciations – Extent
247 and Chronology. Developments in Quaternary Science, vol. 2, Elsevier, Amsterdam, pp.
248 427-445.

249 Kleman, J. and Borgström, I., 1996. Reconstruction of palaeo-ice sheets: the use of
250 geomorphological data. *Earth surface processes and landforms*, 21(10), pp.893-909.

251 Kleman, J., Hättestrand, C., Borgström, I. and Stroeven, A., 1997. Fennoscandian
252 palaeoglaciology reconstructed using a glacial geological inversion model. *Journal of*
253 *glaciology*, 43(144), pp.283-299.

254 Lane, T.P., Roberts, D.H., Rea, B.R., Cofaigh, C.Ó. and Vieli, A., 2015. Controls on bedrock
255 bedform development beneath the Uummannaq Ice Stream onset zone, West
256 Greenland. *Geomorphology*, 231, pp.301-313.

257 Mandryk, C.A., Josenhans, H., Fedje, D.W. and Mathewes, R.W., 2001. Late Quaternary
258 paleoenvironments of Northwestern North America: implications for inland versus coastal
259 migration routes. *Quaternary Science Reviews*, 20(1), pp.301-314.

260 Mann, D.H. and Peteet, D.M., 1994. Extent and timing of the last glacial maximum in
261 southwestern Alaska. *Quaternary Research*, 42(2), pp.136-148.

262 Margold, M., Jansson, K.N., Kleman, J., Stroeven, A.P. and Clague, J.J., 2013. Retreat pattern of
263 the Cordilleran Ice Sheet in central British Columbia at the end of the last glaciation
264 reconstructed from glacial meltwater landforms. *Boreas*, 42(4), pp.830-847.

265 McHenry, M. and Dunlop, P., 2015. The subglacial imprint of the last Newfoundland Ice Sheet,
266 Canada. *Journal of Maps*.

267 Misarti, N., Finney, B.P., Jordan, J.W., Maschner, H.D., Addison, J.A., Shapley, M.D.,
268 Krumhardt, A. and Beget, J.E., 2012. Early retreat of the Alaska Peninsula Glacier
269 Complex and the implications for coastal migrations of First Americans. *Quaternary*
270 *Science Reviews*, 48, pp.1-6.

271 Molnia, B.F., 2008. Glaciers of Alaska. *US Geological Survey professional paper*, (1386K).

272 Sejrup, H.P., Larsen, E., Haflidason, H., Berstad, I.M., Hjelstuen, B.O., Jonsdottir, H.E., King,
273 E.L., Landvik, J., Longva, O., Nygård, A. and Ottesen, D., 2003. Configuration, history
274 and impact of the Norwegian Channel Ice Stream. *Boreas*, 32(1), pp.18-36.

275 Smith, M.J. and Clark, C.D., 2005. Methods for the visualization of digital elevation models for
276 landform mapping. *Earth Surface Processes and Landforms*, 30(7), pp.885-900.

277 Spagnolo, M. and Clark, C.D., 2009. A geomorphological overview of glacial landforms on the
278 Icelandic continental shelf. *Journal of Maps*, 5(1), pp.37-52.

279 Spagnolo, M., Clark, C.D., Ely, J.C., Stokes, C.R., Anderson, J.B., Andreassen, K., Graham,
280 A.G. and King, E.C., 2014. Size, shape and spatial arrangement of mega-scale glacial
281 lineations from a large and diverse dataset. *Earth Surface Processes and*
282 *Landforms*, 39(11), pp.1432-1448.

283 Stokes, C.R. and Clark, C.D., 1999. Geomorphological criteria for identifying Pleistocene ice
284 streams. *Annals of Glaciology*, 28(1), pp.67-74.

285 Stokes, C.R., Tarasov, L., Blomdin, R., Cronin, T.M., Fisher, T.G., Gyllencreutz, R.,
286 Hättestrand, C., Heyman, J., Hindmarsh, R.C., Hughes, A.L. and Jakobsson, M., 2015. On
287 the reconstruction of palaeo-ice sheets: Recent advances and future challenges. *Quaternary*
288 *Science Reviews*, 125, pp.15-49.

289 Storrar, R.D., Stokes, C.R. and Evans, D.J., 2014. Morphometry and pattern of a large sample (>
290 20,000) of Canadian eskers and implications for subglacial drainage beneath ice
291 sheets. *Quaternary Science Reviews*, 105, pp.1-25.

292 Stroeven, A.P., Hättestrand, C., Kleman, J., Heyman, J., Fabel, D., Fredin, O., Goodfellow,
293 B.W., Harbor, J.M., Jansen, J.D., Olsen, L. and Caffee, M.W., 2015. Deglaciation of
294 Fennoscandia. *Quaternary Science Reviews*.

295 Trommelen, M. and Ross, M., 2010. Subglacial landforms in northern Manitoba, Canada, based
296 on remote sensing data. *Journal of Maps*, 6(1), pp.618-638.

297 Trommelen, M.S., Ross, M. and Ismail, A., 2014. Ribbed moraines in northern Manitoba,
298 Canada: characteristics and preservation as part of a subglacial bed mosaic near the core
299 regions of ice sheets. *Quaternary Science Reviews*, 87, pp.135-155.

300

301

Dataset	Horizontal Resolution (m)	Source
Merged on and offshore DEM	500	NOAA
SRTM DEM	30	Earthexplorer.usgs.gov
Landsat ETM+	15 pan-chromatic	Earthexplorer.usgs.gov
IfSAR DEM	5	Earthexplorer.usgs.gov
Adak Bathymetry	30	NOAA
Akutan Bathymetry	12 – 200	NOAA
Chignik Bathymetry	10 - 30	NOAA
Chenega Bathymetry	12	NOAA
Coldbay Bathymetry	12 – 200	NOAA
Cordova Bathymetry	10 – 90	NOAA
Dutch Harbour Bathymetry	15	NOAA
Homer Bathymetry	12 – 200	NOAA
Kachemak Bay Bathymetry	4	NOAA
Kingcove Bathymetry	12 – 200	NOAA
Kodiak Bathymetry	12 – 200	NOAA
Nikolski Bathymetry	30	NOAA
Prince William Sound Bathymetry	4 – 200	NOAA
Sand Point Bathymetry	90	NOAA
Seldovia Bathymetry	30 – 90	NOAA
Seward Bathymetry	4 – 200	NOAA
Tatilek Bathymetry	8	NOAA
Yakutat Bathymery	4 – 200	NOAA

303

304 Table 2. Number of subglacial lineations and streamlined bedrock features per dataset.

Landform type	Data source	Number of landforms
Subglacial lineations	Landsat ETM+	541
	IfSAR DEM	3150
	SRTM DEM	1749
	Offshore Bathymetry	460
Streamlined bedrock	IfSAR DEM	1239

305

306 Table 3. The number of mapped moraines per data set.

Data source	Number of moraine features
Landsat ETM+	514
IfSAR DEM	949
SRTM DEM	1135
Offshore Bathymetry	403

307

308 **Figure Captions:**

309 Figure 1. Overview of the principle palaeo-ice masses in South Alaska. Glacial limits from
310 Alaska Paleo-Glacier Atlas, Version 2 (proposed by Kaufman et al. (2011) and updated from
311 Kaufman and Manley, (2004); www.ncdc.noaa.gov/paleo/alaska-glacier.html). Numbers and
312 boxes show locations of subsequent figures.

313
314 Figure 2. Distribution of datasets used. Coastlines from thematicmapping.org

315
316 Figure 3. Subglacial lineations (drumlins) near Becharof Lake. (A) SRTM hill-shaded DEM,
317 illuminated from the NW. Arrow denotes approximate palaeo-ice flow direction. (B) SRTM hill-
318 shaded DEM, this time illuminated from the NE. (C) Landsat false colour composite of the same
319 drumlins. (D) Mapped subglacial lineation outlines.

320
321 Figure 4. Examples of glacially streamlined bedrock. Arrows denote approximate palaeo-ice
322 flow direction. (A) Hill-shaded IfSAR DEM of bedrock lineations West of Talkeetna,
323 Matanuska-Susitna Borough. (B) Hill-shaded IfSAR DEM of a mixture of streamlined bedrock,
324 crag and tails, and sediment lineations, near McKinley Fall, Matanuska-Susitna Borough.
325 Regions of bedrock highs correspond to subglacial lineations with a qualitatively different
326 morphology, thought to be streamlined bedrock.

327
328 Figure 5. Examples of moraine mapping. (A) Hill-shaded SRTM DEM of prominent moraines of
329 both the Cordilleran Ice Sheet and the Akhlun Mountains Ice Cap. (B) Derived mapping. Note

330 how the areas of looping moraines denoted by polygons also have prominent ridges mapped as
331 polylines. Kvichak Bay begins to the south east of these images.

332

333 Figure 6. Examples of Alaskan subglacial lineations. Arrows denote palaeo-ice flow direction.

334 (A) Lineations within McCarthy Borough, dissected by the Chitina River. (B) Elongate

335 lineations near the confluence between the West and East Forks of the Yetna River. (C) Hill-

336 shaded STRM DEM of subglacial lineations (drumlins) on the valley floors of the Akhlun ice

337 cap. This example depicts the area near lakes Nerka, Aleknagik and Nunavaugaluk. (D) Hill-

338 shaded bathymetry of submerged subglacial lineations, SE of Mitrofanina Bay.

339

340 Figure 7. Examples of Alaskan moraines. Arrows denote palaeo-ice flow direction and terminate

341 at the moraines. (A) Hill-shaded SRTM DEM of moraines at the heads of Morzhovoi Bay (left)

342 and Cold Bay (east). (B) Hill-shaded SRTM DEM of moraines north of the Alleutians, north of

343 Mother Goose lake. (C) Hill-shaded SRTM DEM of concentric looped moraines, related to the

344 Akhlun ice cap, east of Tikchik Lake. (D) Hill-shaded IfSAR DEM of moraines north of Mt.

345 Denali.

346

347 Figure 8. Examples of eskers and meltwater channels on hill-shaded IfSAR DEMs. (A) A large

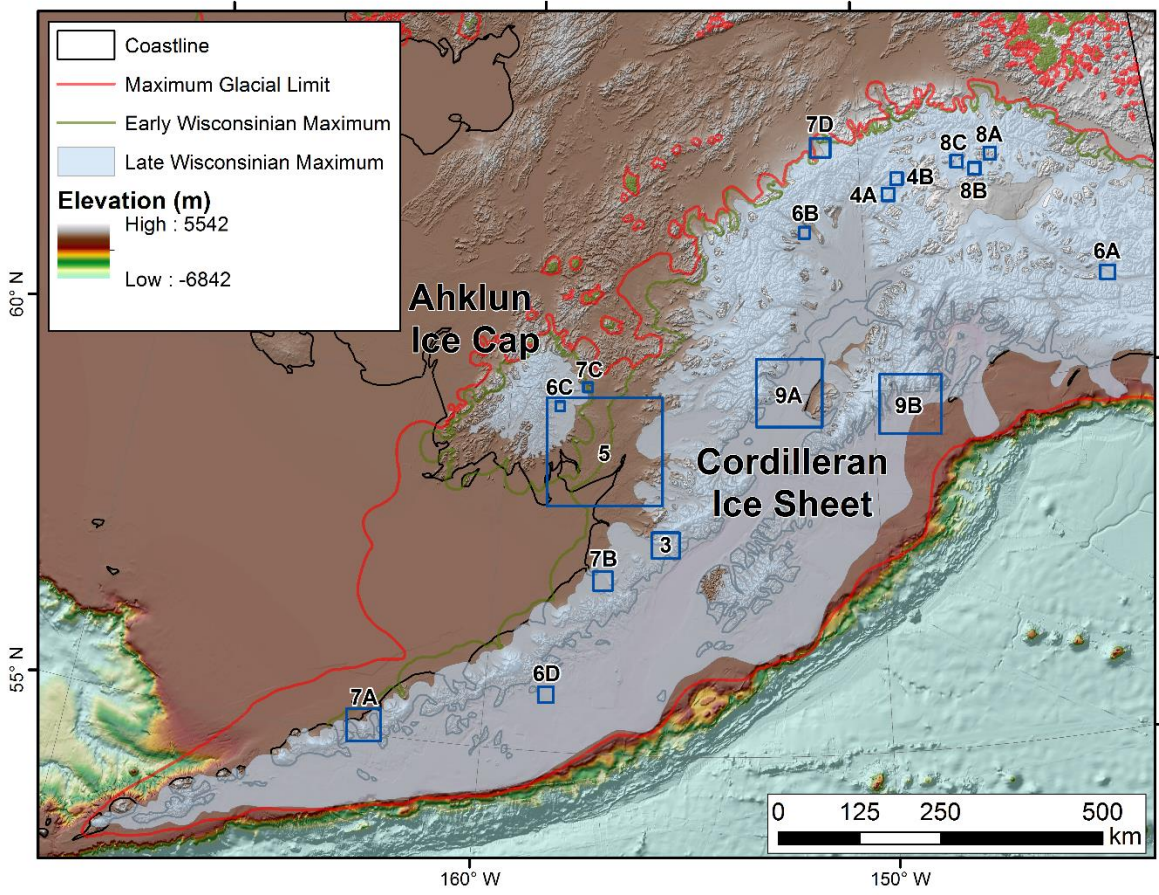
348 esker, passing through Lower Tangle Lake, Paxson. (B) An esker which grades into a meltwater

349 channel, west of Dickey Lake, Valdez-Cordova. (C) A series of meltwater channels, located

350 along the Denali Highway, east of Alpine Creek Lodge.

351

352 Figure 9. Examples and profiles across glacially occupied troughs. Images are hill-shaded
353 merged bathymetry and elevation data. (A) The Shelikof Strait. (B) Troughs and fjords, south of
354 Kenai Fjords National Park. (C) Profiles across lines Y to Y' and Z to Z', located on (A) and (B).
355

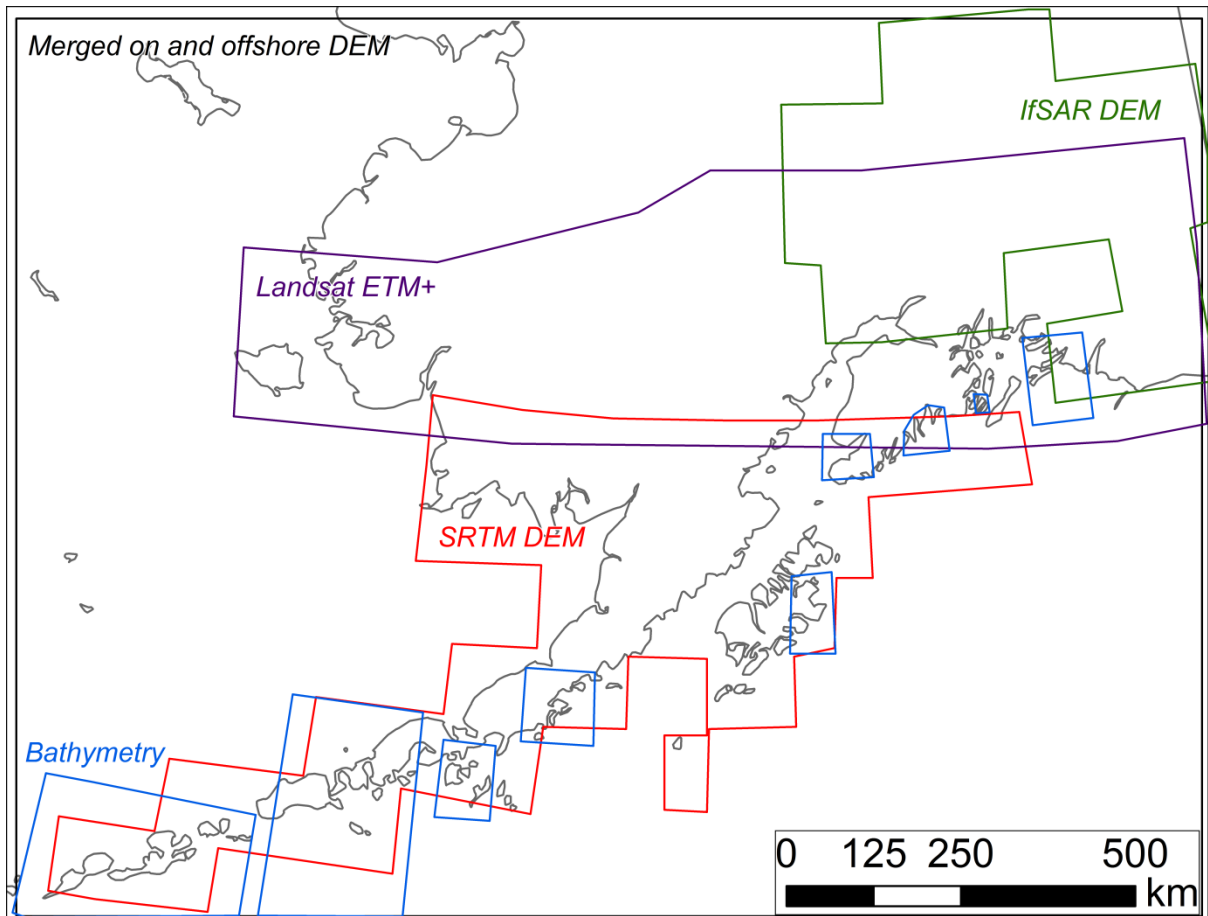


357

358

Figure 1

359

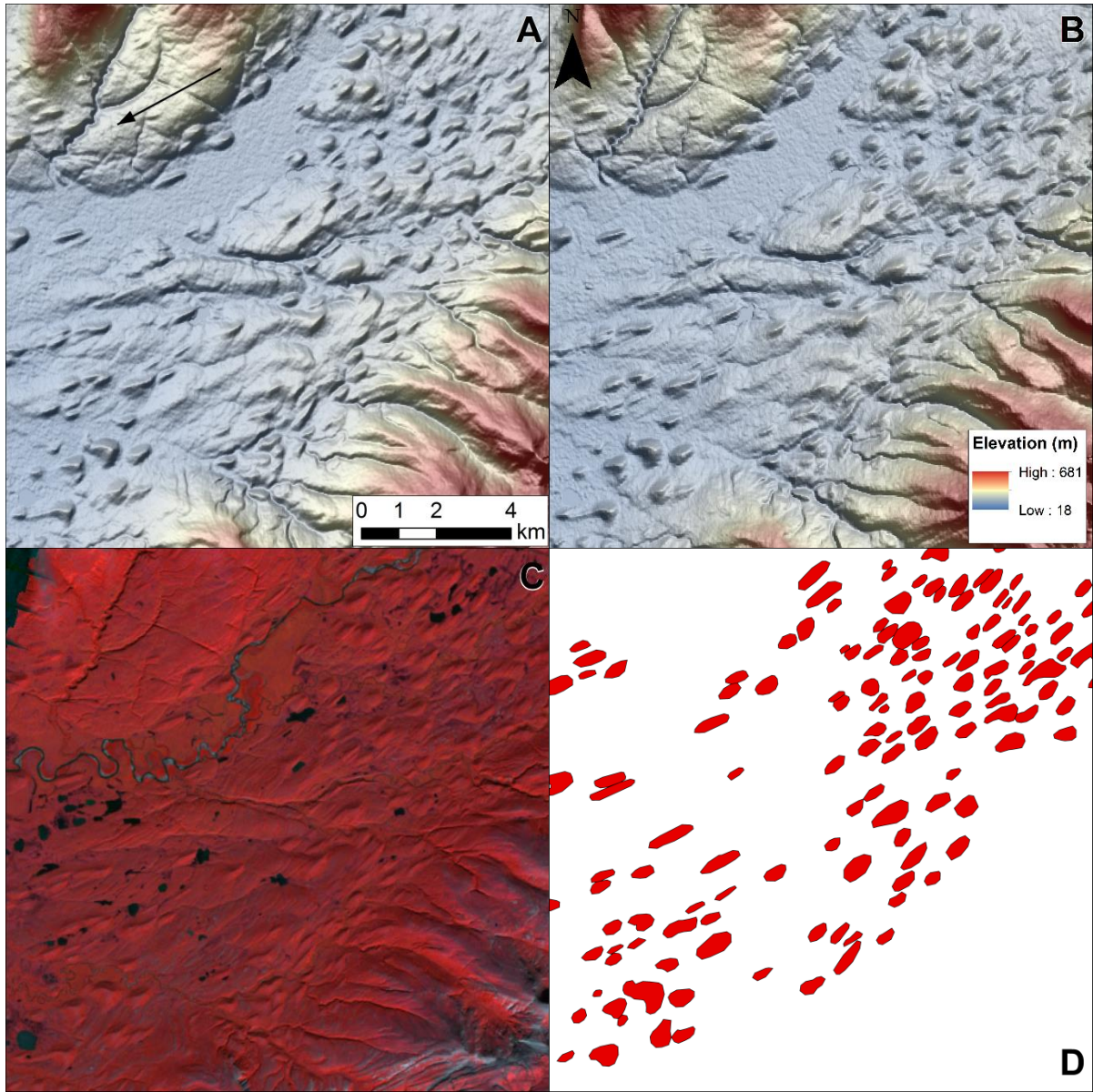


360

361

362

Figure 2



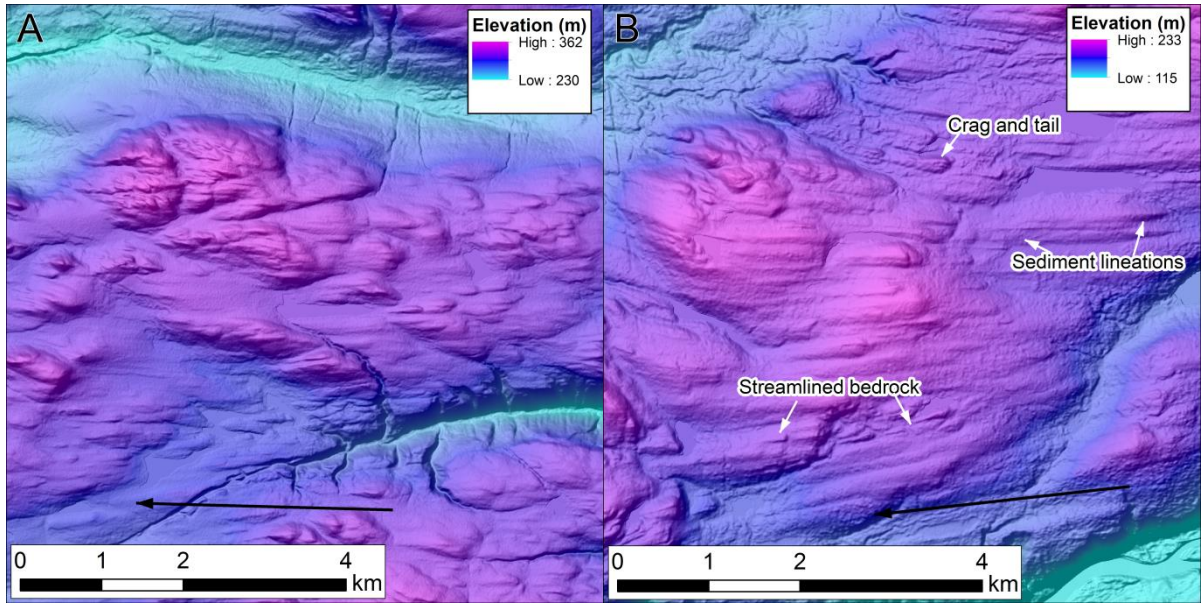
363

364

365

366

Figure 3

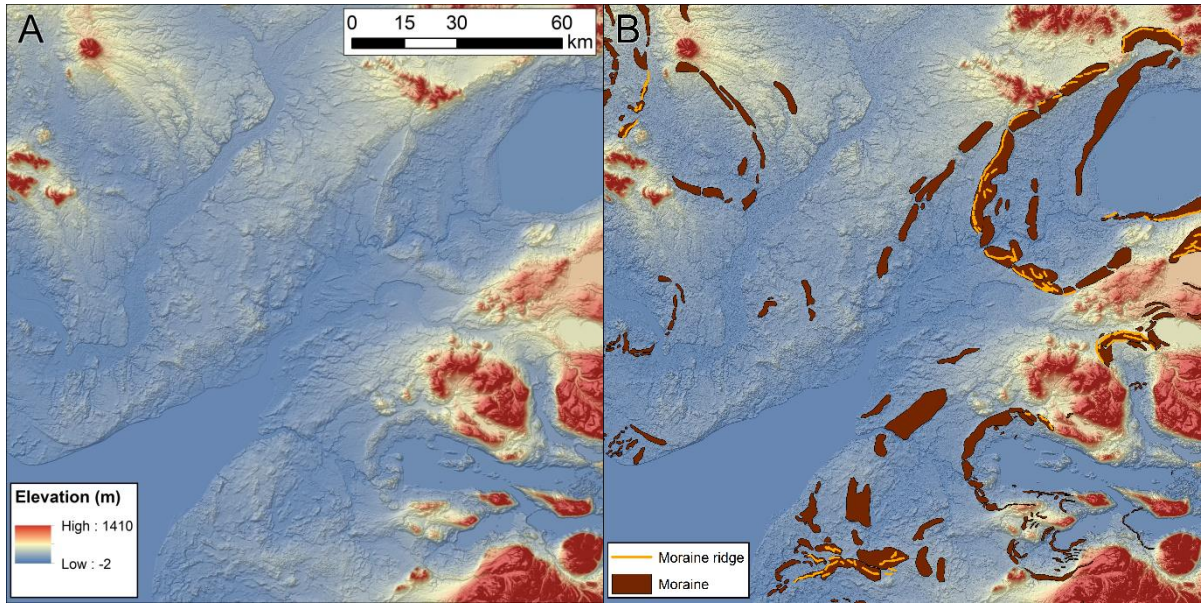


367

368

369

Figure 4



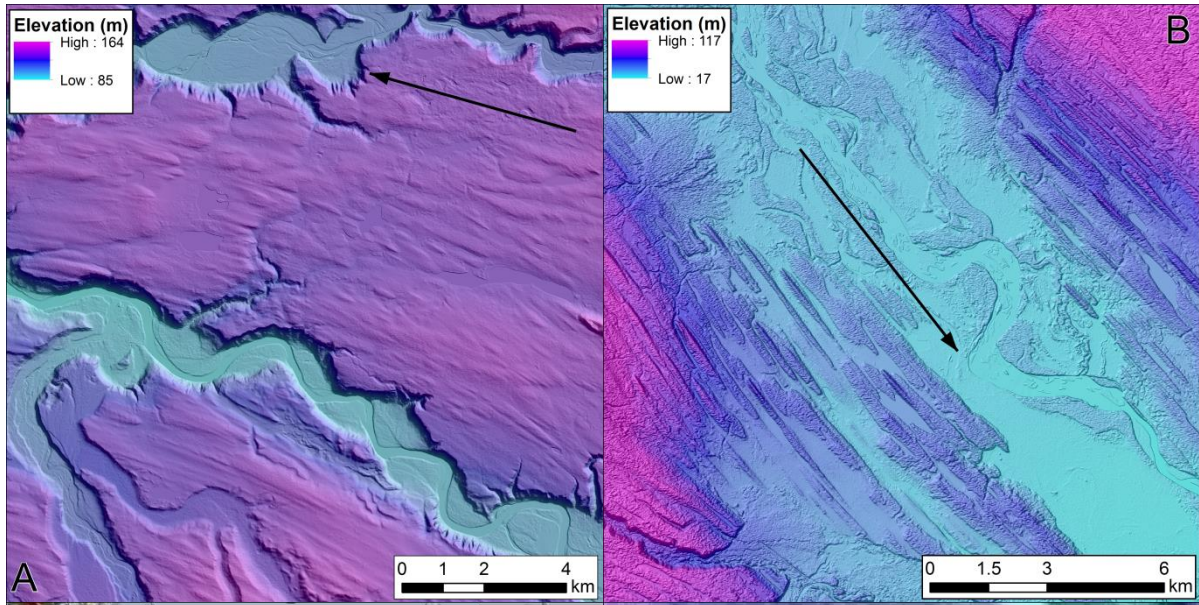
370

371

372

Figure 5

373



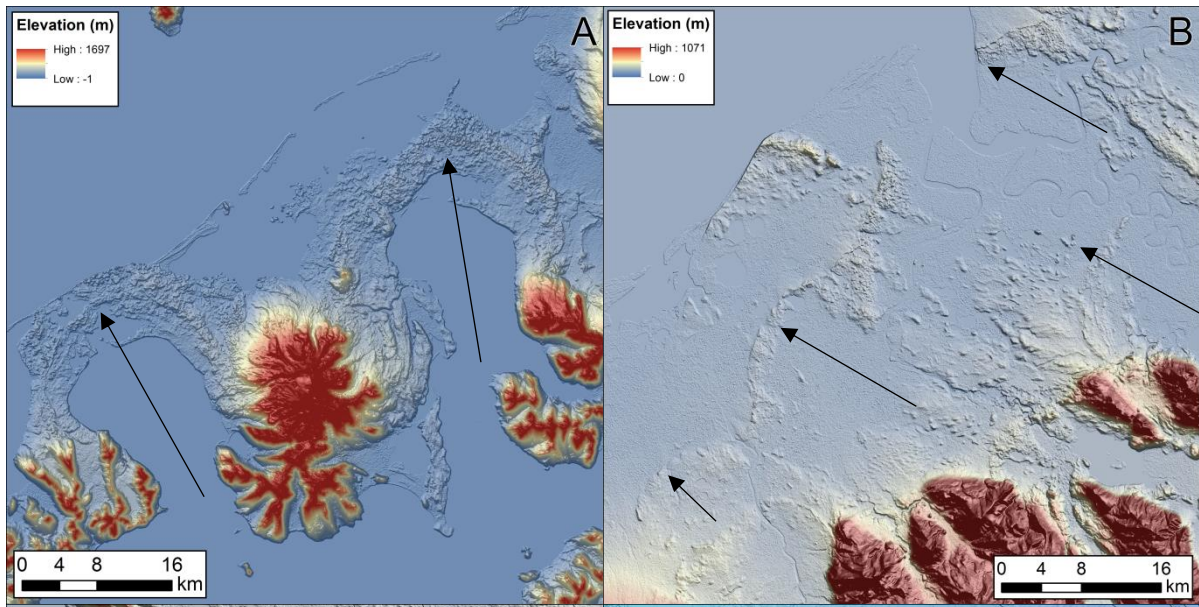
374

375

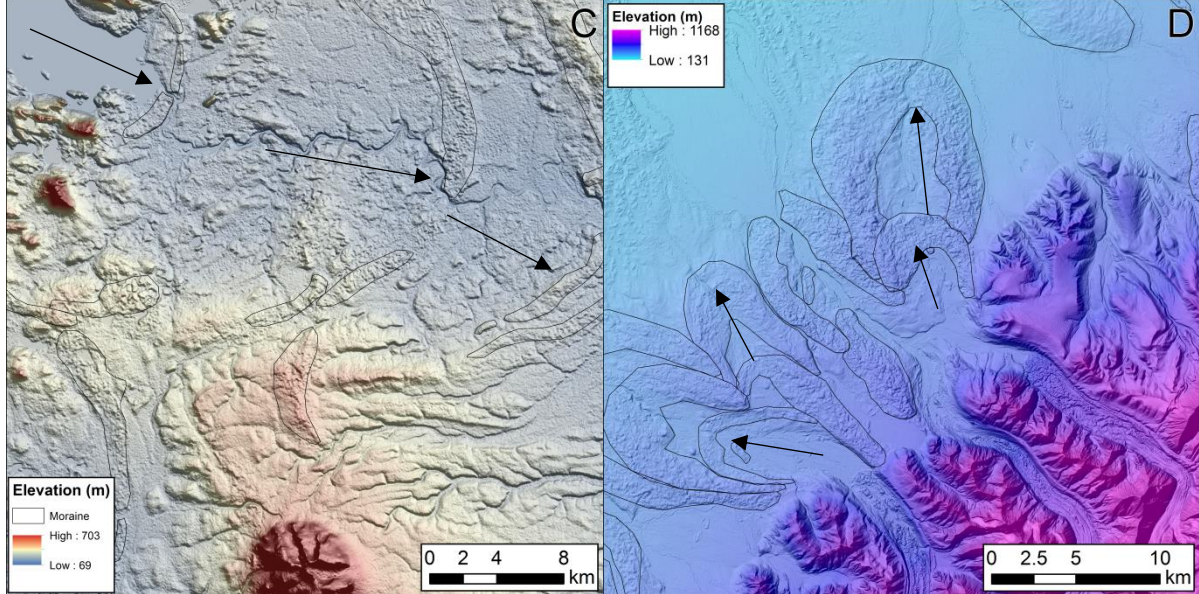
376

Figure 6

377



378

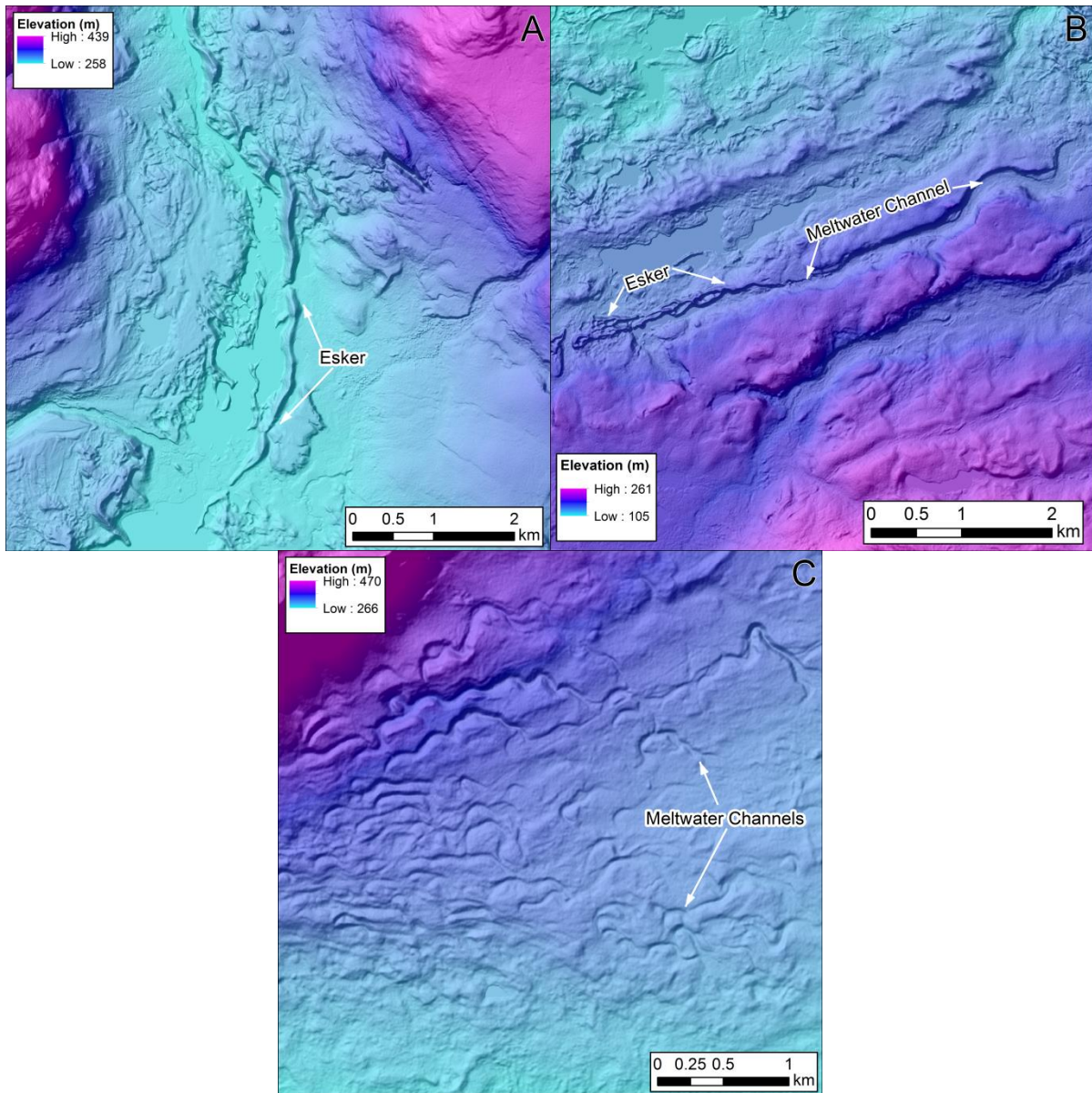


379

Figure 7

380

381

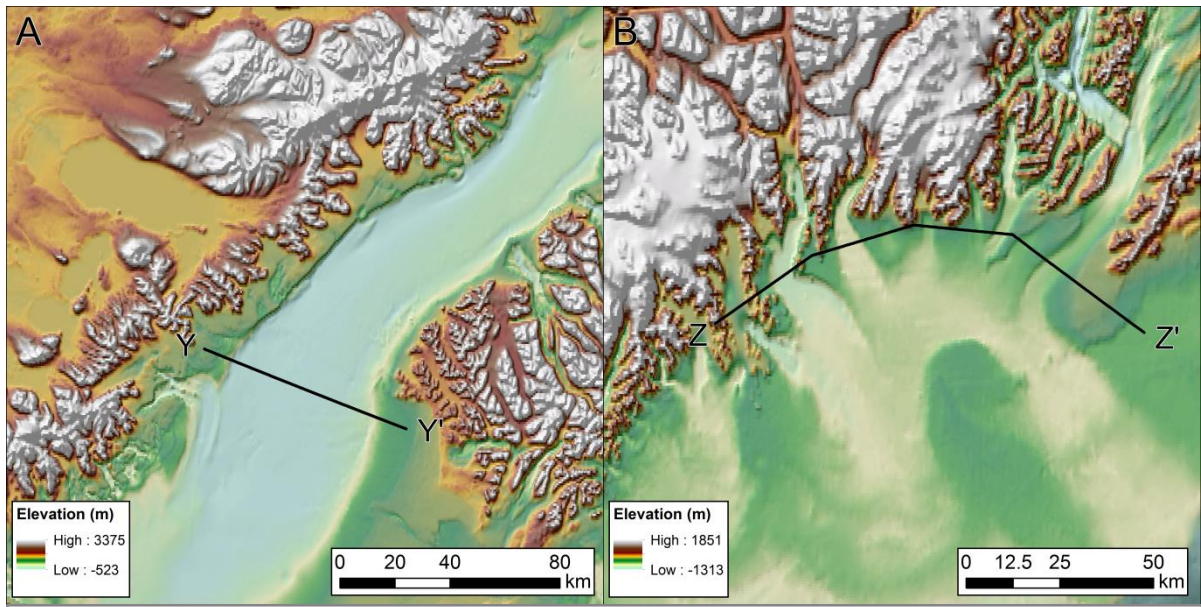


382

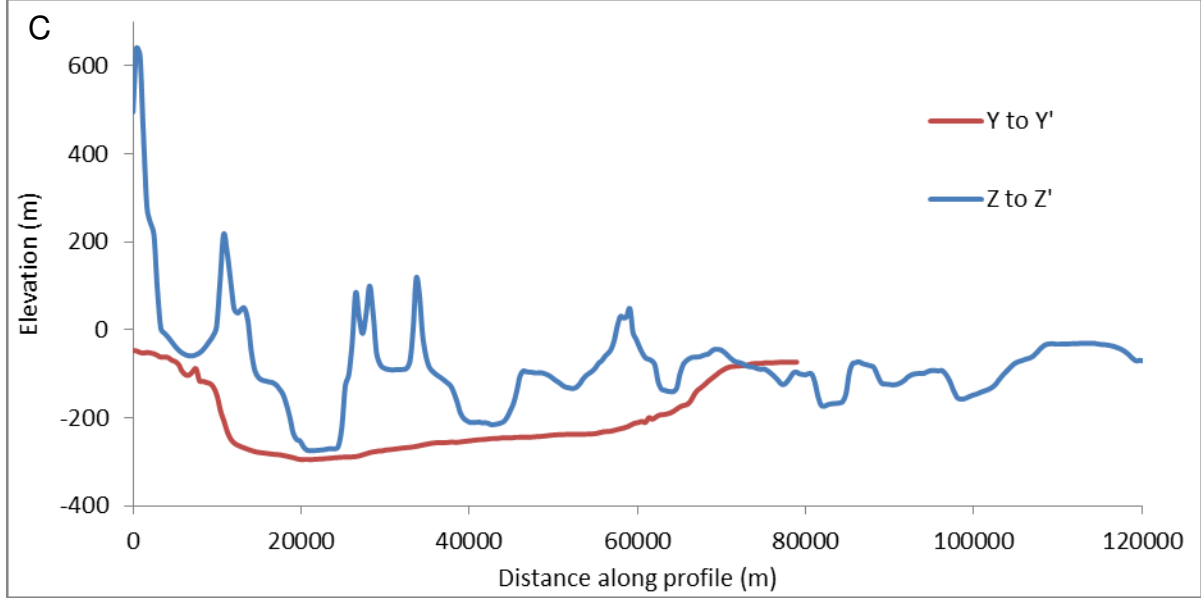
383

384

Figure 8



385



386

387

388

389

390

Figure 9